Chemosphere
March 2024, Volume 352 Pages 141487 (12p.)
https://doi.org/10.1016/j.chemosphere.2024.141487
https://archimer.ifremer.fr/doc/00879/99054/

Practical guidelines for representing and interpreting rare earth abundances in environmental and biological studies

Barrat Jean-Alix [1, 2, *], Bayon Germain [3]

[1] Univ Brest, CNRS, Ifremer, IRD, LEMAR, Institut Universitaire Européen de la Mer (IUEM), Place Nicolas Copernic, 29280, Plouzané, France

[2] Institut Universitaire de France, Paris, France

[3] Univ Brest, CNRS, Ifremer, Geo-Ocean, F-29280, Plouzané, France

* Corresponding author : Jean-Alix Barrat, email address : barrat@univ-brest.fr

This paper summarizes the main guidelines for representing rare earth element (REE) abundance patterns, along with a review of the common mistakes or omissions that can alter REE plots and bias interpretations. It is specifically designed for ecotoxicologists and biologists, for whom the study of these elements has become an important field of research in recent years. Prior to applying REE diagrams to the study of living organisms, it is important to understand the rationale that led geochemists and cosmochemists to develop them. Used with the practical recommendations described here, these diagrams have the capacity to highlight fundamental processes taking place in the biosphere.

Graphical abstract

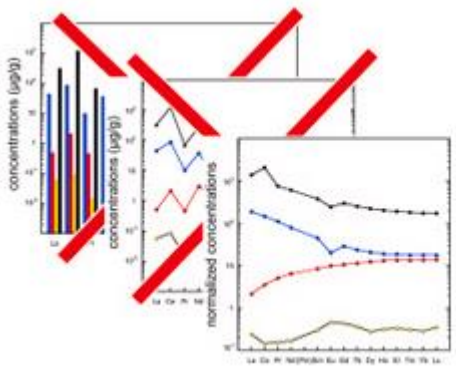

Highlights

► Rationale behind the use of REE normalization. ► Misuse and common errors in drawing REE patterns. ► REE patterns of living organisms show promising perspectives.

Keywords : Rare earth elements, Oddo-harkins effect, REE pattern, Normalization values, REE anomalies

1/ Introduction

Rare earth elements (REEs) are a group of fifteen elements - the lanthanides (La, Ce, Pr, Nd, Pm, Sm, Eu, Gd, Tb, Dy, Ho, Er, Tm, Yb, Lu), with Z values ranging from 57 to 71, to which chemists commonly add Y (Z=39) and sometimes Sc (Z=21), although the latter has a very different geochemical behavior. Apart from Pm, which is radioactive, with a very short half-life (only 2.62 y), and is therefore absent in nature, these elements are not so rare and typically occur in trace amounts in most rocks. Over the past 60 years, REEs have become one of the most studied groups of elements in Earth and Universe Sciences. It is beyond the scope of this paper to enumerate all the diverse applications offered by REEs. Just as an example, the behavior of the REEs during magma genesis is well understood, so their abundances can be used in petrological studies to provide constraints on the formation of both terrestrial and extraterrestrial rocks. Additionally, REE are powerful proxies to investigate both present and past surface processes, in both marine and continental environments, for characterizing and tracing ocean water masses (e.g., Garcia-Solsona et al., 2014), but also estuarine processes (e.g., Elderfield et al., 1990), groundwater mixing (e.g., Johannesson et al., 1997; Noack et al., 2014), and for understanding carbon sequestration (e.g., Karamalidis et al., 2012), acid mine drainage (Prudencio et al., 2015), and in-situ remediation of groundwater (e.g., Wilkin et al., 2021). Furthermore, the radiogenic isotopic compositions of REE (i.e. Nd, Ce) are now well-established tools for dating rock formation, in provenance studies, and to reconstruct the evolution of geochemical reservoirs during our planet's history (e.g., Henderson, 1984).

The tremendous interest drawn for rare earths by cosmochemists, geochemists and geologists over the last decades is in stark contrast to the much more recent attention paid to these elements in life sciences. In contrast to most geological samples, REE abundances in organisms are generally very low. It is only very recently that these elements have been shown to participate in biochemical cycles, particularly in methanotrophic organisms (e.g., Pol et al., 2014; Semrau et al., 2018). Apart from these recent discoveries, the potential use of REEs by organisms remains largely unknown. While evidence exist for REE accumulation in certain organisms (e.g., Ozaki et al., 1997) and for their utility in promoting plant growth (e.g., Ouyang et al., 2003), the mechanisms involved in the biological use of REE are still poorly understood. Substantial research effort will be required in future years on the above-mentioned subjects, especially as these elements are nowadays brought into the environment by human activities. Since the 1970s, the industrial demand for REEs has grown

exponentially. These metals have become highly strategic (e.g., Hatch, 2012; Massari and Ruberti, 2013) and are now indispensable in many critical fields, such as electronics, manufacturing of magnets (e.g., for wind turbines), batteries, oil refining (fluid-cracking catalysts), polishing medias, and medical imaging. A corollary of this markedly increasing consumption of REE is the emergence of new pollution pathways linked to the extraction, purification and use of these elements, and above all to the production of new waste (e.g., Brewer et al., 2022). This raises new questions for the environmental sciences and biology: how can we identify and quantify the pollution generated by these elements? What are the impacts of these emerging pollutants on the environment and on living organisms? To answer these questions, but also to understand how these elements may be transferred from nutrients to organisms, from one organ to another, but also on another scale from one trophic level to another, diagrams need to be developed by biologists and ecotoxicologists. Such diagrams, known as REE-patterns, are widely used in geochemistry and cosmochemistry. Not only do they enable REE abundances to be visualized, they can also be used to detect enrichment or depletion of certain REEs relative to neighboring elements and corresponding so-called 'anomalies'. The aim of this paper is to introduce the basic principles of these diagrams first developed for applications in Earth Sciences, but showing great potential in the fields of biochemistry and ecotoxicology.

2/ A few words on analytical techniques

Over the past 60 years, considerable progress has been made in determining REE abundances in rocks and water. Most analytical techniques have been applied with varying degrees of success, depending on the type of sample. Until the 1990s, these techniques were not routinely capable of determining all REEs. They also required complex equipment, and were frequently time-consuming and laborious. For example, neutron activation, which was a major analytical technique, required the use of a nuclear reactor (neutron source) to irradiate samples, and the use of scintillation-type detectors to record the spectra of radioactive emissions to calculate element concentrations at different times after irradiation. Several counting stages, spaced several tens of days apart, and sometimes several months, were required to obtain La, Ce, Nd, Sm, Eu Tb, Yb and Lu (e.g., Chayla et al., 1973). At the time, the most accurate measurement technique was isotope dilution combined to thermal ionization mass spectrometry (ID-TIMS; e.g., Schnetzler and Philpotts, 1968; Gast et al., 1970). Samples in solution were spiked with a solution containing artificial REEs whose compositions were

very different from those of natural REEs. The REEs in the spiked sample were separated using ion exchange columns, then their isotopic compositions were measured using solid-source mass spectrometry. This technique solely allowed measurement of the concentrations of polyisotopic rare earths (La, Ce, Nd, Sm, Eu, Gd, Dy, Er, Yb, Lu), albeit with very high accuracy (RSD<2-3%). It was nevertheless time-consuming, since one day of measurement was required to determine the REE concentrations of any single sample by single-collector mass spectrometry at that time. Additionally, prior to analysis, the time needed to prepare a series of samples could approach 3 weeks, including rock dissolution, beaker washing and decontamination, and chemical separations.

Other techniques such as inductively coupled plasma - atomic emission spectrometry (ICP-AES) were subsequently developed, enabling REEs to be determined simultaneously and more rapidly (e.g., Walsh et al., 1981; Watkins and Nolan, 1992). While this technique is still used by some laboratories, ICP-AES instruments were superseded in the late 1990s by the development of inductively coupled plasma-mass spectrometry (ICP-MS), enabling all REEs to be determined, with very low detection limits (e.g., Jenner et al., 1990; Jarvis and Jarvis, 1992) and generally much improved accuracy for low-level samples characterized by low REE concentrations.

With the advent of ICP-MS, the acquisition of high-quality data with accuracies equivalent to those yielded by isotopic dilution techniques in the 1990s has now become routinely accessible and fast, with analytical costs being much lower than with neutron activation or ID-TIMS. Nowadays, the time required to analyze a sample for REE concentrations by ICP-MS only takes a few minutes (excluding sample preparation time). Almost all REE data are now acquired by ICP-MS.

In contrast to most geological materials, biological samples are commonly depleted in REEs, with concentrations for these elements typically in the range of a few ng/g to tens of ng/g for some of them (e.g., Danezis et al., 2019 and references therein). As a consequence, the analysis of biological samples for REE is even more difficult than for rocks displaying the lowest REE abundances. Regarding the analytical measurement of REE by ICP-MS, two important points have to be emphasized:

-First, particular care needs to be taken regarding measurement quality and instrumental conditions, as isobaric interferences can be generated in the plasma. These interferences are capable of generating significant concentration anomalies that can result in biased measured

abundances. As for the geological samples, REE interferences should be systematically monitored and corrected during every ICP-MS analytical session. Eu concentrations cannot be determined correctly if isobaric Ba oxide interferences are not properly estimated and corrected. This type of artifact is known for plants (Pourret et al., 2022), and is particularly critical for samples displaying high Ba/REE ratios. It can be easily detected using Eu/Sm vs. Ba/Sm diagrams (Fig. 1). The reader is referred to Zepeda et al. (2023) for a recent discussion.

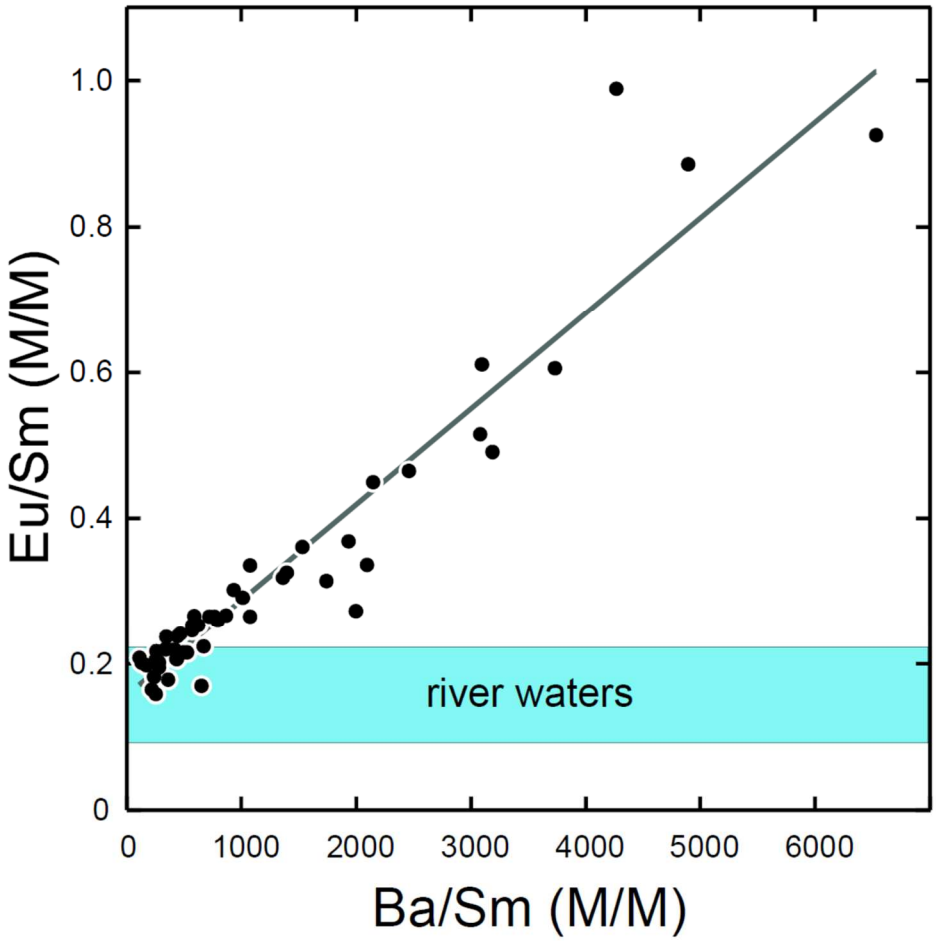

Figure 1. Eu/Sm vs. Ba/Sm plot for waters from St. Lawrence River (Dang et al., 2022). Measurements were obtained by ICP-MS. Eu/Sm ratios correlate with Ba/Sm ratios (r=0.95). Such a relationship indicates that Eu concentrations are affected by isobaric BaO interferences generated in the plasma, and are mostly incorrect. Dang et al. (2022) also analyzed a control standard with satisfactory results. This standard (SLR6) has a Ba/Sm ratio of around 400, too low to detect the effect of interferences.

In samples showing extremely high Ba/REE ratios, isobaric interferences can even affect Sm and possibly Gd abundances. Apart from these particular samples, interference corrections are generally successful for determining reliable and accurate Eu abundances. Alternatively, the use of ICP-MS instruments equipped with collision cells that can efficiently break up complex molecules formed in the plasma can quantitatively reduce isobaric interferences. Additionally, high-resolution sector field ICP-MS offers the capability of resolving REE ion signals from their isobaric interferences. Despite these advantages, these techniques cannot be applied to REE-poor samples, since they typically result in a drastic decrease of signal intensity by two orders of magnitude. Moreover, they do not generally produce better quality results than those obtained at low resolution with interference correction for regular samples (Charles et al., 2021). Therefore, for Ba-rich samples, the best solution to overcome interference issues is to separate Ba from the REEs prior to analysis. Several methods have been proposed and successfully applied routinely for REE-depleted samples (e.g., Barrat et al., 1996, 2020; Bau et al., 2010).

Similarly, the oxides and hydroxides of light REEs and middle REEs formed in the plasma must be evaluated and accounted for during analytical sessions, as they correspond to isobars of the isotopes monitored to determine Gd and heavy-REE concentrations, hence possibly leading to overestimation of their measured abundances. This problem is particularly critical in the case of Gd pollution studies (see below).

-Second, a large number of certified reference materials for geological materials now exist, for which very precise and accurate REE concentrations have been determined. Among these, two basaltic materials - BHVO-2 (Hawaii) and BCR-2 (Colombia River) - are among the best characterized geological standards (Jochum et al., 1996) available at present. Unfortunately, there are currently no biological standards as precisely characterized for REE abundances. This lack of standard represents one major limitation for the validation of REE determinations in biological studies. Moreover, organic matter can be depleted in REEs by several orders of magnitude compared to associated detrital material (e.g., soil, sediment, dust, oxides). As a result, some biological standards may contain minute amounts of inorganic (terrigenous) matter, much enriched in REEs, which can affect measured REE abundances depending on the procedures used for sample preparation and digestion. The "duckweed" reference standard (BCR 670) is a good example of this problem (Zocher et al., 2021). The preparation of a rock powder is of course very different from that of organic matter, but it will be important for biological studies in the future to have access to well-characterized ‘organic’ reference

materials for REE abundances, as well some of the precisely characterized geostandards (e.g., BCR-2 or BHVO-2). This would validate observed anomalies and facilitate intercalibration of results between different laboratories worldwide. Biologists must bear in mind that, behind the questions of bioaccumulation and vital effects, the REEs contained in well-prepared samples of organisms originate from their living environments, and that consequently, the distributions observed in organic matter are largely inherited from those found in ambient water and sediments. Therefore, any REE 'anomaly' identified in biological samples can only be directly attributed to vital effects or anthropogenic contributions providing that interferences and calibration have been properly assessed during analysis.

3/ Why is the behavior of REEs so coherent and why do some REEs decouple from the rest of the group?

REEs are remarkable in many respects. First, their atoms have complex electronic configurations, with a 4f electronic sublayer filling in from Ce to Lu. Under terrestrial conditions, these elements are generally trivalent. The consequence of these electronic configurations is that their ionic radius decreases linearly with the number of elemental charges (Fig. 2). This contraction in ionic radius is known to chemists as "lanthanide contraction". From La^{3+} to Lu^{3+}, effective ionic radii (coordination number VIII) change from 1.16 (La) to 0.977 Å (Lu), a variation of only 18.7% (Shannon, 1976). Between two consecutive elements, effective ionic radii vary by only 0.8 to 1.5 %. As the chemical behavior of ions is largely controlled by charge (3+ here), and ionic radius, these variations explain on the one hand the consistency of the chemical behavior of trivalent REEs in nature, but also the impossibility for natural processes to specifically decouple one of these elements from its neighbors. Consequently, the abundances of two neighboring trivalent REEs (e.g., Pr and Nd, Gd and Tb, Tb and Dy, Dy and Ho, Ho and Er, etc.) are generally highly correlated in nature, and the linear relationships obtained between these pairs of elements are therefore useless, and provide no constraint for discussing/discriminating the processes that might be responsible for variations in abundance as exemplified in Figure 3.

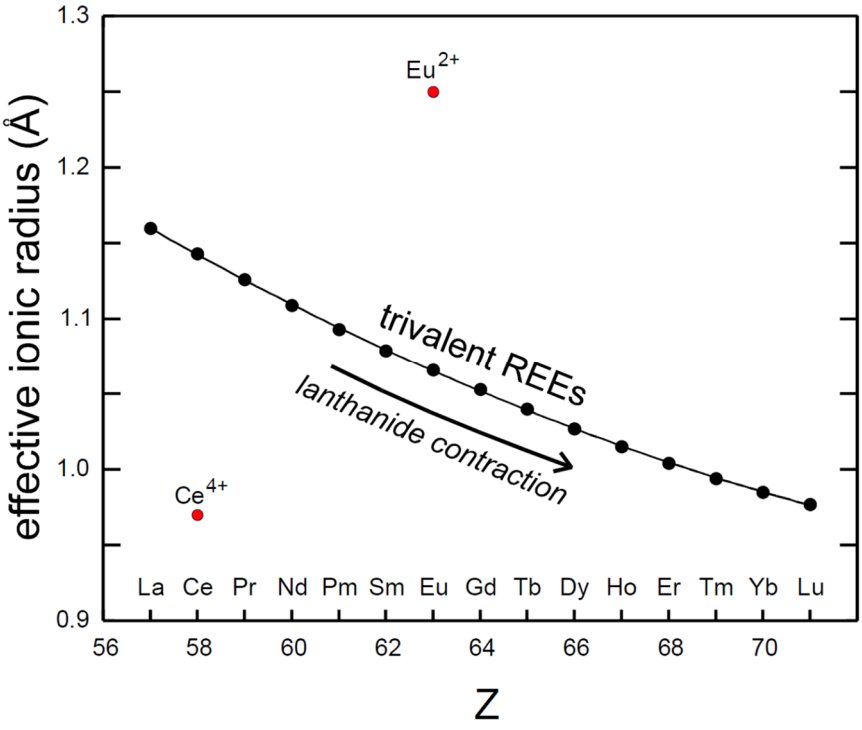

Figure 2. Effective ionic radii vs. atomic numbers (Z) for REE in VIII coordination (Shannon, 1976).

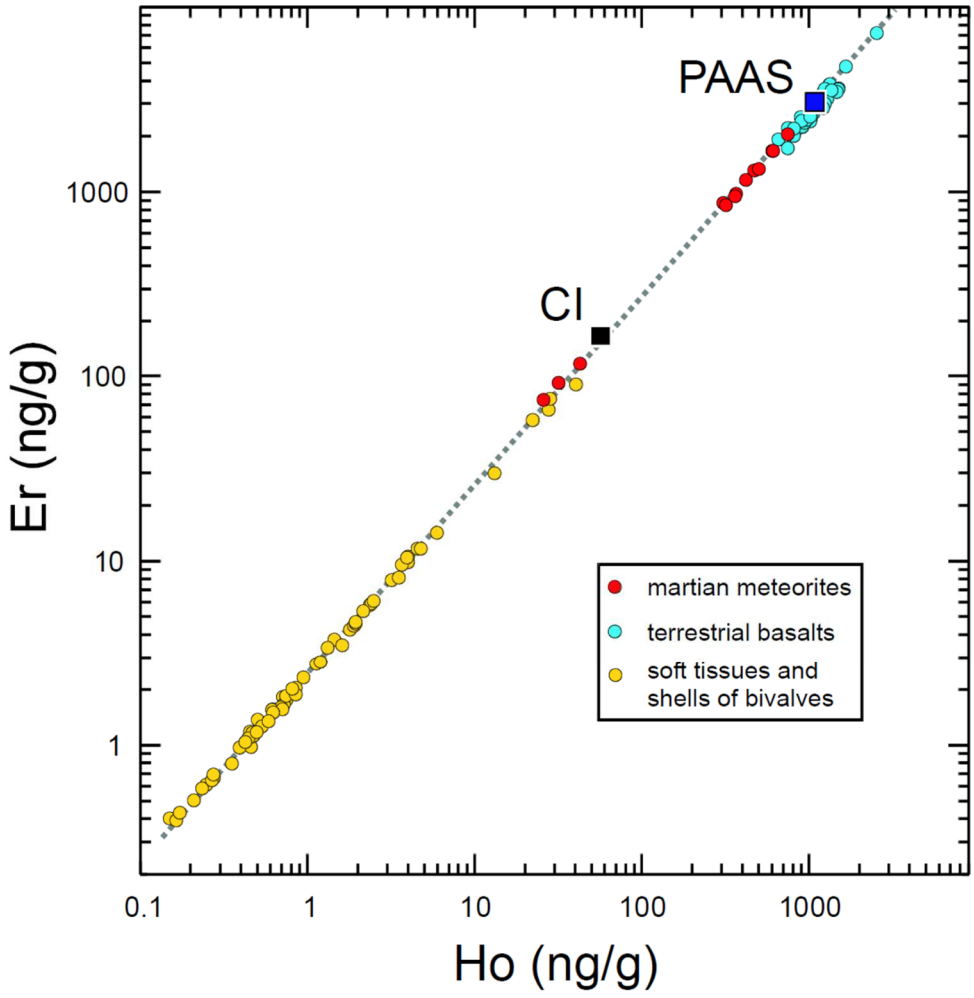

Figure 3. Er vs. Ho plot for Martian rocks, terrestrial basalts, bivalves (soft tissues and shells), CI chondrite and post-archean shale average (PAAS). All the data were produced in the same laboratory and selected in order to avoid any analytical bias (Barrat et al., 2012, 2016, 2022b) except the shale average (Pourmand et al., 2011). All analyses lie on the same line, controlled by the chondritic (CI) Er/Ho ratio. A wide variety of processes produced the observed abundance ranges, but did not decouple these two elements. Obtaining a straight line in this diagram does not discriminate between different processes or sample origins, since samples that have absolutely nothing to do with each other are always on this line.

Natural abiotic processes can modify the relative proportions of REE abundances. For example, the partial melting of rocks in the Earth's mantle will produce lavas enriched in REE compared to corresponding parental rocks, generating enrichments in the lightest REEs. These enrichments will not be specific to any single element, but progressive and a function of the element's charge number (Z) or ionic radius. Such gradual enrichments can be modeled in order to infer magma formation models for example (e.g., Minster and Allègre, 1978).

241 However, specific decoupling of particular elements from the other REEs is naturally possible
242 on Earth, essentially for the following elements: La, Ce, Eu and Y.

243 Europium and Ce can have different valences, and therefore exhibit distinct behavior
244 in Earth's systems. During magma genesis, depending on oxygen fugacity, Eu can be present
245 in two valence states, Eu^{2+} and Eu^{3+} (e.g., Goldschmidt, 1958). Europium^{2+} has an ionic
246 radius similar to that of Ca^{2+}, and can therefore be substituted for this element in the crystal
247 lattice of calcic minerals. Cerium is always trivalent during magma genesis, but in aquatic
248 environments, it can be oxidized and become tetravalent (e.g., Goldberg, 1961). This property
249 explains the distinctive behavior of Ce in oceans (e.g., German and Elderfield, 1990). This
250 decoupling of Ce from the other REEs is an extremely useful tool for reconstructing redox
251 environmental changes over the Earth's history (e.g., Tostevin et al., 2016; Wallace et al.,
252 2017; Bellefroid et al., 2018 and references therein).

253 In life sciences, the possibility of significant biological fractionation of REEs has only
254 been considered recently. Biological effects on REE abundances can be hampered by
255 environmental signals. For instance, thiotrophic mussels living in the vicinity of submarine
256 hydrothermal vents typically show significant excess in Eu abundances, which reflect the
257 composition of hydrothermal fluids (Bau et al., 2010; Barrat et al., 2022a). Nevertheless, Ce
258 fractionation linked to biological activity has been recently, as demonstrated by Kraemer and
259 Bau (2022). Filter-feeding bivalves (dog cockles, *Glycymeris glycymeris*) also indicate
260 significant Ce fractionation that co-varies with the age of the animals, hence suggesting a
261 possible metabolic link (Barrat et al., 2022b). These studies are promising and call for further
262 in-depth investigation of the mechanisms driving biological fractionation in living organisms.

263 Lanthanum excess is typically observed in seawater and in various chemical
264 precipitates, in which this particular characteristic can be used as a diagnostic feature of a
265 seawater origin (e.g., Bau and Dulski,1996a; Kamber and Webb, 2001). Lanthanum has been
266 suggested to be more stable than other light REEs during complexation in seawater (de Baar
267 et al., 1985) or to be preferentially released from suspended barite particles (Grenier et al.,
268 2018). None of these explanations is fully satisfactory. Recently, it has been discovered that
269 La is used by methanotrophic organisms (e.g., Pol et al., 2014, Semrau et al., 2018). These
270 microbes convert methane into methanol, then into formaldehyde, using methanol
271 dehydrogenase enzymes. Some methanotrophic organisms use lanthanide-dependent enzymes
272 to produce formaldehyde. This enzymatic activity is capable of generating La anomalies and
273 other light-REE enrichments in marine organisms (Wang et al., 2020; Bayon et al., 2020;

Barrat et al., 2022a), which can potentially impact REE abundances in surrounding water (Shiller et al., 2017). Recent experimental work has also demonstrated the activity of Eu as an enzymatic cofactor in the methanotrophic bacterium *Methylacidiphilum fumariolicum* (Jahn et al., 2018). Lanthanide-dependent methanotrophy is currently the only natural process known to significantly fractionate REEs from each other, but its potential importance in the marine REE budget remains to be investigated.

As for REEs, Y (which is not a lanthanide) is also trivalent in nature and has the same ionic radius as Ho^{3+}. Unsurprisingly, the behavior of these two elements is identical in a wide range of environments. In fact, these elements are generally considered as geochemical twins. The Y/Ho ratios in most chondrites, achondrites, Martian, lunar and terrestrial rocks (magmatic and terrigenous sediments) vary within a very limited range of values (~27.7 ± 2.7; Bau, 1996; Pack et al., 2007). However, in aquatic environments, Y is generally strongly decoupled from Ho partly due to different complexation behavior onto suspended particulates (e.g., Bau et al., 1997; Nozaki et al., 1997). As a result, measured Y/Ho ratios for seawater and seawater-derived precipitates (carbonates, Fe-Mn crusts) significantly depart from chondritic or solid-Earth values, meaning that Y/Ho can be used as a tool to discriminate the relative contribution of marine versus terrestrial REE signatures in environmental and biological samples (e.g., Kamber et al., 2001).

4/ REE and REY patterns

In the universe, elements with an even Z number greater than 6 (i.e. carbon) have higher abundances than their immediate neighbors with an odd Z value. This property, known as the Oddo-Harkins effect, is a consequence of nucleosynthesis, the origin of chemical elements. Rare earths are no exception to this rule, and their relative abundances in nature are largely inherited from primordial distributions. Geochemists realized early on that, in order to interpret and visualize REE abundances in samples, it was necessary to find a way of representing the data that would erase the Oddo-Harkins effect and enable enrichments or depletions of REEs to be highlighted in relation to a reference. We owe the creation of REE patterns to Masuda (1962) and Coryell et al. (1963). Their principle is very simple: REE concentrations in a sample are normalized to the abundances of a chosen reference material (Table 1).

Table 1. Preferred normalization values. The chondrite (CI) is obtained from 5 g of the Orgueil meteorite (Barrat et al., 2012). This value is preferred to other compilations due to the large mass used. The sediment average (PAAS) is that obtained by Pourmand et al. (2011) and has been adjusted to the values of the standards obtained in Brest. Note that the Y/Ho ratio of the CI chondrite is 27.5, and that the calibration we use is in agreement with the values of the standards given by Jochum et al. (2016). The concentrations are given in µg/g and µmol/kg.

	CI-chondrite	CI-chondrite	PAAS	PAAS
unit	µg/g	µmol/kg	µg/g	µmol/kg
Y	1.56	17.55	32.2	362
La	0.235	1.692	44.75	322.2
Ce	0.600	4.28	87.29	623
Pr	0.091	0.646	10.1	71.68
Nd	0.464	3.22	36.98	256.4
Sm	0.153	1.018	6.908	45.94
Eu	0.0586	0.386	1.188	7.818
Gd	0.206	1.31	5.958	37.89
Tb	0.0375	0.236	0.894	5.625
Dy	0.254	1.563	5.272	32.44
Ho	0.0566	0.343	1.078	6.536
Er	0.166	0.992	3.094	18.50
Tm	0.0262	0.155	0.468	2.77
Yb	0.168	0.971	3.028	17.5
Lu	0.0246	0.141	0.438	2.503

The resulting ratios or "normalized concentrations" are plotted from La to Lu following increasing atomic number Z (Fig. 4). As the reference also has elemental distributions reflecting the Oddo-Harkins effect, the latter disappears, and a smooth curve is obtained that enables small differences in the fractionation of one REE from another to be identified graphically. Pioneering authors of this representation chose a reference chondritic material for normalization.

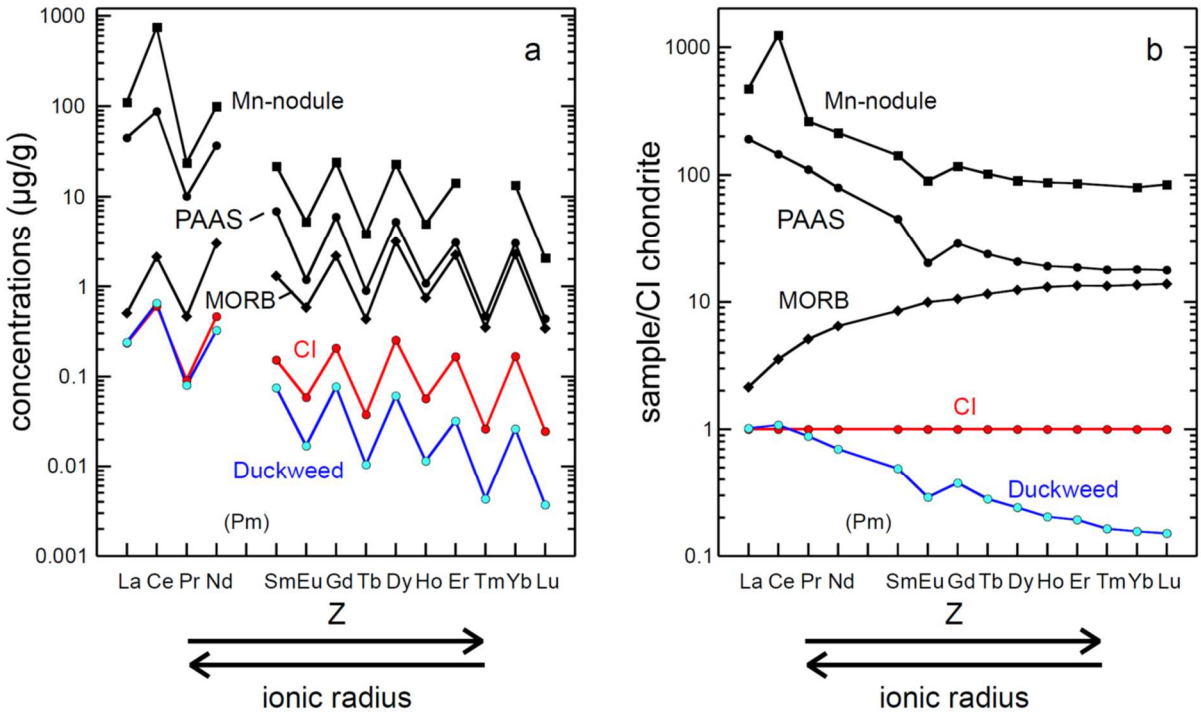

Figure 4. a/ Unnormalized REE pattern (a) and chondrite normalized REE pattern for the reference CI chondrite, a mid-ocean ridge basalt (MORB), the reference post-archean Australian shale average (PAAS), a Mn-nodule, and a duckweed sample. The x-axis corresponds to the atomic number of the elements (Z), which are linked to the ionic radii (the ionic radius increases with decreasing Z, see figure 2). The non-normalized patterns have a sawtooth shape characteristic of the Oddo-Harkins effect. They are uninterpretable, as enrichments and anomalies cannot be identified. Note that Pm is lacking in natural samples and cannot be placed in figure 4a. REE patterns display a segment connecting Nd and Sm normalized concentrations by convention (Fig. 4b).

There were several reasons for this choice. First, chondrites are primitive meteorites, whose REE concentrations are proportional to those of the solar photosphere, hence considered to represent the bulk Solar System for these elements, and the building blocks of planets. This reference is therefore universal, and can be used for all types of extraterrestrial or terrestrial materials, including biological objects. Second, this representation can be used to highlight "enrichments" or "depletions" in certain groups of REEs, commonly referred to as light REEs (from La to Sm, “LREE”), middle REEs (Sm, Eu and Gd, “MREE”), and the heavy REEs (from Gd to Lu, “HREE”). Let us pause for one moment to clarify what these words mean, which have nothing to do with the level of REE abundances in relation to the reference. Whatever the REE abundances of any sample are, this particular sample will be considered as being enriched in light REEs if normalized abundances decrease from La to Sm. This

enrichment can be quantified with the La_n/Sm_n ratio (also noted as $(La/Sm)_n$; with *n* stating for 'normalized'), which in this case is >1. Conversely, a sample will be considered as being depleted in light REEs when its normalized abundances increase from La to Sm, hence characterized by $(La/Sm)_n<1$. The same definitions equally apply to heavy REE; a sample enriched in heavy REE will display a $(Lu/Gd)_n$ ratio greater than 1, and vice versa. In Figure 3, we have plotted some patterns of typical rocks. The mid ocean ridge basalt (MORB) is depleted in light REE compared to the reference chondrite, even though its REE abundances (including light REEs) are much higher than those of chondrites. The average shale (Post Archean Australian Shale or PAAS; Taylor and McLenann, 1985) is enriched in light REE but not in heavy REEs.

The resulting REE patterns can be used to highlight the decoupling of certain REEs such as La, Ce and Eu from neighboring REE, the calculation of which will be explained below. It should be emphasized here that raw (unnormalized) REE abundance patterns do not allow to read all the information they carry. Therefore, these plots are obsolete and should not be used anymore. When describing REE patterns normalized to a set of reference values, we are of course interested in the level of concentrations relative to this reference. We also attach great importance to the general shape of the patterns, which may display any depletion, enrichment, concavity or convexity, relative to the reference material used for comparison. These REE characteristics can be quantified, and along with concentration levels, are parameters that can be used to test models concerning rock formation, or the origin of REEs accumulated in organisms.

Geochemists working on sediments, waters and, more generally, surface processes, prefer to use a reference other than chondrites to normalize their data. They generally use average values for post-Archean terrigenous sediments such as shales or muds, hence with geologic age < 2.5 billion years old (this is because the oldest Archean continental crust was significantly different in composition; e.g. Taylor and McLennan, 1985). Over the past decades, different set of values for terrigenous sediments have been proposed and used for REE normalization purposes, which are known by the following acronyms: PAAS (Nance and Taylor, 1976; Taylor and McLennan, 1985), NASC (Gromet et al., 1984), MUQ (Kamber et al., 2005), WRAS and WRAC (Bayon et al., 2015), EUS (Bau et al., 2018). All these references serve the same purpose. Their REE abundances may slightly vary from one set of values to another, but they are generally taken as being representative of the general REE composition of the upper continental crust, hence displaying concentration ratios presumably

very close to those for this geochemical reservoir. Standardizing data with such a reference is particularly recommended when investigating the geochemistry of sediments or sedimentary rocks (including marine precipitates) and natural waters (river and marine waters), because their REE abundances are directly inherited from the upper continental crust. Therefore, the shape of the REE pattern obtained with this type of reference material makes it easier to visualize elemental decoupling during Earth surface processes or chemical precipitation in natural waters. Importantly, these sedimentary references do not display any significant anomaly in La or Ce compared to chondrites, and consequently do not result in particular bias when calculating corresponding anomalies for these elements, whose values obtained are similar to those calculated with chondrites (Barrat et al., 2023). Like the upper continental crust, these sediments are enriched in light REE and have a negative Eu anomaly relative to chondrites. Therefore, REE normalization using sediment reference values offers the advantage of improving the visualization of REE patterns for soils, continental sediments, marine sedimentary rocks and natural waters, but they may also blur particular Eu anomalies inherited from crustal reservoirs. Europium is trivalent in Earth surface environments, and the observed variability for Eu abundances in the above-mentioned sample types cannot be explained by a change in its valence. In practice, all the sedimentary references mentioned above are equally valid, and give similar REE patterns. While the choice of one or any other set of reference values may vary in different laboratories worldwide, the most widely used sediment reference for REE is PAAS, which corresponds to the average values of a dozen of post-Archean shale samples from Australia, as initially proposed by Nance and Taylor (1976) and Taylor and McLennan (1985), and recently re-determined using high-quality REE measurements by Pourmand et al. (2011). Concentrations of an element X normalized to one of these references are generally noted as X_{sn} (« sn » standing for « shale normalized »). X_n is used for normalization with a chondritic reference.

This type of normalization using sediment reference values is also best suited for biological samples, since the REEs they contain are de facto of crustal origin, even for those samples formed in seawater. Instead, the use of any organic material for normalization purpose would most likely complicate the interpretation of resulting REE patterns.

One typical oversight that is made today by some geochemists and cosmochemists is the omission of Pm from the other normalized REE elements to be plotted on the x-axis. The x-axis does not correspond to a list of elements, but to the atomic number (Z) of the elements, which here varies from 57 (La) to 71 (Lu). The omission of Pm (Z=61) produces a jump from

Nd (Z=60) to Sm (Z=62), and a local change in the shape of the pattern that can be significant. The cause of this mistake is simple. When REE data were initially produced using techniques that did not allow all the REEs present in the samples to be determined, analysts plotted the elements using the correct 'distances' between them. Nowadays, the use of ICP-MS techniques generally allows all the REEs to be analyzed in samples. Since Pm is a radioactive element with a very short half-life (a few years), it is virtually non-existent in nature, and therefore cannot be measured. It is consequently absent from the list of elements supplied by analysts, and is therefore commonly forgotten when REE patterns are drawn. The omission of Pm in normalized REE patterns can lead to errors when calculating anomalies (see below), and hence should be avoided.

Yttrium can also be added to the elements to be represented in normalized REE patterns. As discussed above, Y has a similar valence and ionic radius as Ho, and hence can be inserted between Dy and Ho. This addition is likely to modify the smoothness in the heavy-REEs portions of the patterns. However, the advantage of being able to highlight Y-Ho decoupling, particularly in aquatic environments, largely offsets this drawback. These patterns are known as Rare Earth and Y (REY) patterns (e.g., Bau and Dulski, 1996a). We would like to draw readers' attention to a calibration problem. While there is good agreement on standard REE concentrations, state-of-the-art data diverge slightly on Y abundances. There is a small analytical bias between laboratories for this element, which can be higher than 10 %. This is illustrated by the average Y/Ho ratios (concentrations in µg/g) obtained by various laboratories for international basalt and granite standards: 27.73 (σ = 1.16, n=19), Jochum et al. (2016); 25.34 (σ = 0.55, n=6), Pourmand et al. (2011); 23.63 (σ = 0.61, n=8), Makishima and Nakamura (2006). We therefore recommend to check the standard results and choose normalization values that are compatible with the calibration of the results that the reader wishes to normalize.

In principle, there are two types of vertical scale (y-axis) that can be used for representing normalized REE patterns: a linear scale or a logarithmic scale. The use of a logarithmic scale is often justified by the fact that normalized concentrations may vary over several orders of magnitude. This is true, but not the only essential reason. Unlike linear scales, logarithmic scales preserve elemental ratios independently of their abundances. To illustrate this, rather than to discuss it mathematically, we have chosen to use a simple example. In Figure 5, we have plotted the REE pattern of a seawater sample, and theoretically calculated the patterns of the same seawater diluted with pure water. Such dilution obviously

results in reduced abundances, but it should not change corresponding elemental ratios. The results obtained are plotted using both a linear and a logarithmic scale. The patterns all display different shapes in the linear scale, but are perfectly parallel in the logarithmic scale. This example illustrates the fact that the shapes of the patterns can only be compared using a logarithmic scale. The use of a linear scale should hence be avoided. The only case a linear scale could be used would be when one wants to compare samples with very similar normalized abundances. But even there, the usefulness of using a linear scale for the y-axis would be objectively debatable.

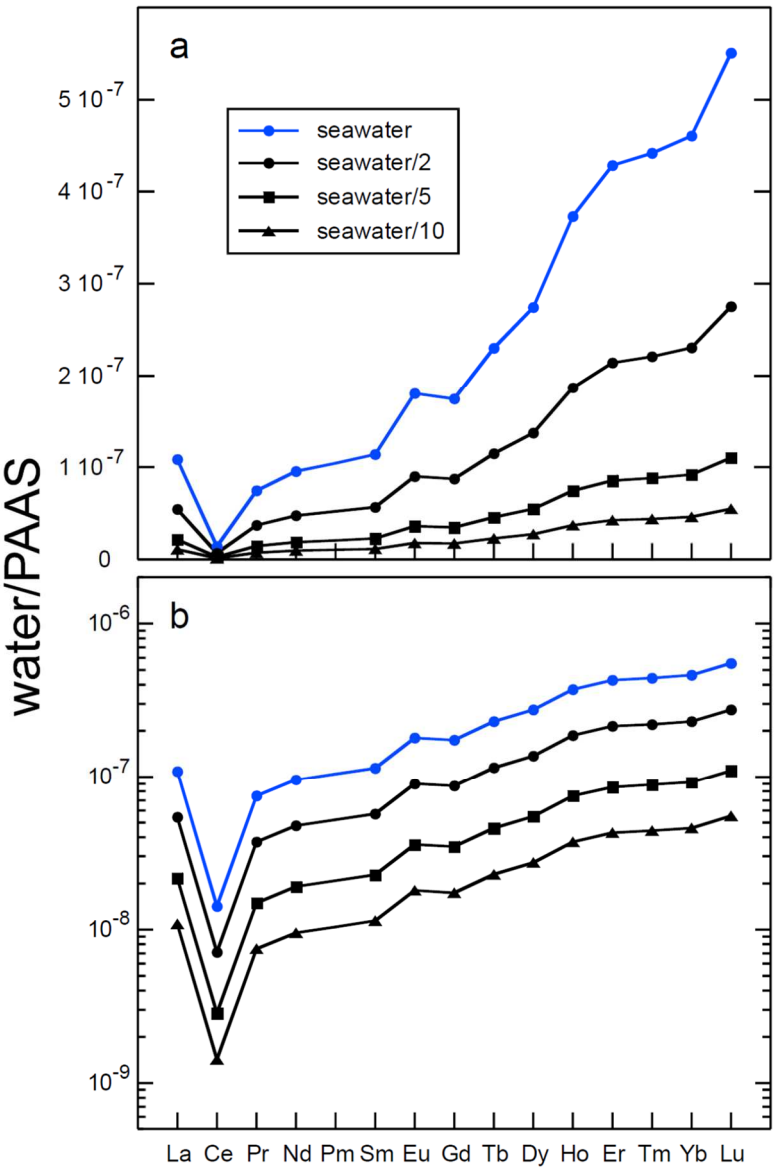

Figure 5. REE patterns of calculated mixtures between a theoretical seawater sample and pure water plotted using a linear (a) and a logarithmic scale (b). See text for discussion.

5/ Calculation of REE anomalies: La, Ce, Eu, Y.

One of the interests of REE patterns is to highlight the different behavior of certain elements relative to their immediate neighbors. This decoupling can be estimated using the ratio X/X*, where X is the measured concentration of the element, and X* its theoretical concentration as estimated assuming a smooth REE pattern (i.e. a pattern in which three neighboring REEs would be perfectly aligned). A positive anomaly occurs when any element X is in excess in the sample (X/X*>1), and a negative anomaly when it is in deficit (X/X*<1).

X* can be determined in many different ways, and has been the subject of much development in the literature. The reader is referred to the work of Lawrence et al. (2006) for a thorough synthesis of possible equations for estimating X*. There are two philosophies for estimating X*: 1/ by interpolating or extrapolating X* linearly, which implies reasoning with REE patterns having concentrations represented using a linear scale; or 2/ by interpolating or extrapolating X* geometrically, hence considering an y-axis with a logarithmic scale. Both ways are still used by the Earth and environmental sciences community. This issue has been discussed in detail recently, showing that linear interpolations or extrapolations could lead to erroneous results for REE anomalies (Barrat et al., 2023). Even if they are still being used routinely in certain fields (e.g., marine geochemistry), these linear estimations are not rigorous, and should be avoided. Instead, geometric interpolations or extrapolations should be preferentially used when calculating REE anomalies. Figure 6 illustrates how La, Ce and Eu anomalies are calculated. The recommended equations are listed below using concentrations normalized to a chondritic reference (X_n), but the same equations also apply for normalization to a shale material (X_{sn}).

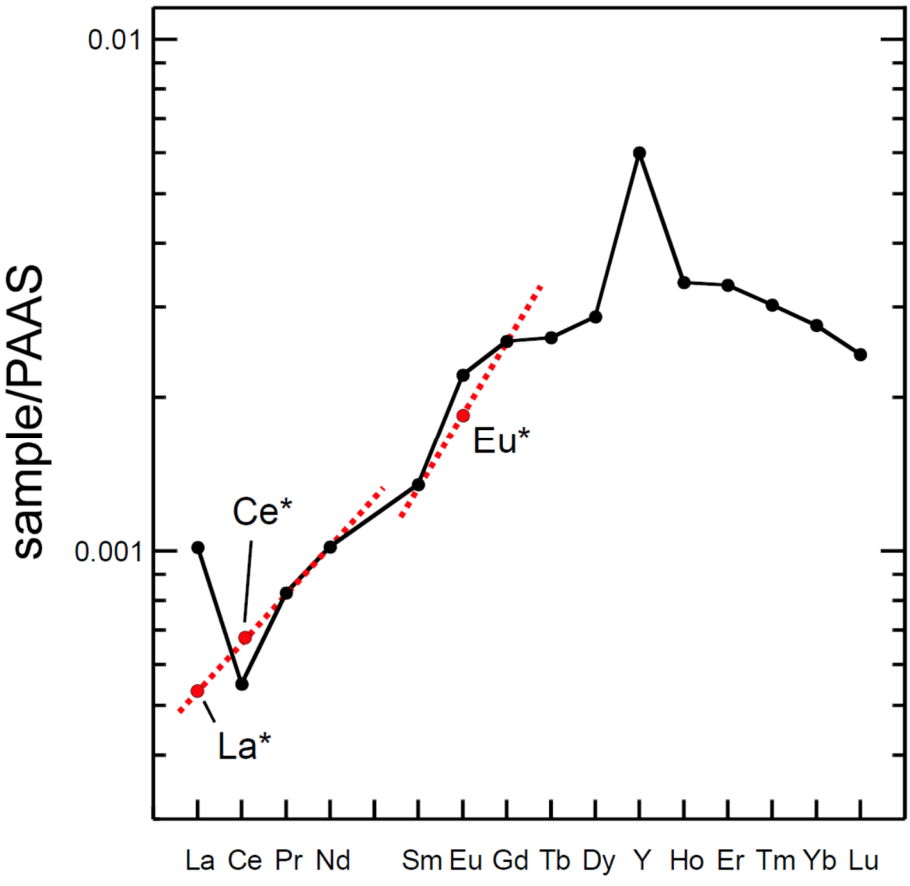

Figure 6. REY pattern of a coralline algae showing how La*, Ce*, and Eu* are estimated. Note that the y-axis is logarithmic.

The Eu anomaly is the most straightforward to calculate. Europium is placed between Sm and Gd. If there is no anomaly for these elements (i.e., no pollution), Eu* can be estimated using their geometric mean:

$$Eu/Eu^* = Eu_n/(Sm_n \times Gd_n)^{1/2} \quad \text{(equation 1)}$$

Similarly, if there is no anomaly in La, we can calculate the anomaly in Ce in the same way by interpolating Ce* using the geometric mean of the normalized abundances of La and Pr :

$$Ce/Ce^* = Ce_n/(La_n \times Pr_n)^{1/2} \quad \text{(equation 2)}$$

However, this equation is not recommended due to the frequent presence of a La anomaly, particularly in marine or oceanic environments. Geometric extrapolation of Ce* from Pr and Nd abundances is recommended:

$$Ce/Ce^* = Ce_n \times Nd_n / Pr_n^2 \quad \text{(equation 3)}$$

If Pr is not determined, this anomaly can also be estimated by interpolating Ce* with Nd and Sm. The calculation is made using the correct distance between Sm and Nd, and is only rigorous if Pm has not been omitted. The equation is then:

$$Ce/Ce^* = Ce_n \times Sm_n / Nd_n^2 \quad \text{(equation 4)}$$

The way to estimate La* is similar, and this concentration can be extrapolated from Pr and Nd concentrations:

$$La/La^* = La_n \times Nd_n^2 / Pr_n^3 \quad \text{(equation 5)}$$

In the case of REY patterns, the Y anomaly is calculated with the Y/Ho ratio because these elements have the same ionic radii (remember that Z-value are on the x-axis, and that Z-value variations are equivalent to ionic radius variation for REEs) This ratio is calculated directly with normalized or non-normalized concentrations. The usual practice is to calculate the Y/Ho ratio using raw concentrations expressed in the same unit (i.e., ng/g or µmol/l). As this number is dimensionless, it is important to specify the units in which the concentrations are expressed.

6/ REE anomalies in polluted samples

Two cases of REE pollution can be considered here, depending on whether the pollutant display a regular REE pattern or not. One example is the case of REE pollution linked to the production of phosphate fertilizers (e.g., Gaudry et al., 2007). The effluents discharged by this industry produce a non-uniform increase in the concentrations of all the REEs, without creating anomalies that are unknown in natural samples. In this case, data processing and estimation of the anomalies do not require any specific calculations. The previous equations apply. However, human activities may also generate REE pollutions related to the use of products specifically containing certain purified REEs such as e.g. permanent magnets (Nd, Dy, Pr, Tb), petroleum fluid catalytic cracking (FCC) catalysts (La, Ce), polishing (La, Ce), alloys (La, Ce, Pr, Nd, Gd), rechargeable batteries (light REEs), glasses and ceramics (La, Ce, Pr, Er, Y), medical imaging (Gd). The consumption of REEs is growing exponentially and anthropogenic REE pollution is now well documented for Gd (e.g., Bau and Dulski, 1996b), La and Sm (e.g., Kulaksiz and Bau, 2011, 2013). The REE patterns have made it possible to identify them thanks to the resulting anomalies produced.

Pollution by other REEs will inevitably be detected in the coming years. To be quantified, the use of REE patterns and the calculation of anomalies (X/X*) will have to be well mastered, particularly in the field of environmental sciences and ecotoxicology. Examples of patterns of samples polluted with Gd, La and Sm will be briefly discussed here to illustrate the principles of anomaly calculation, which can be transposed for other REEs in the future.

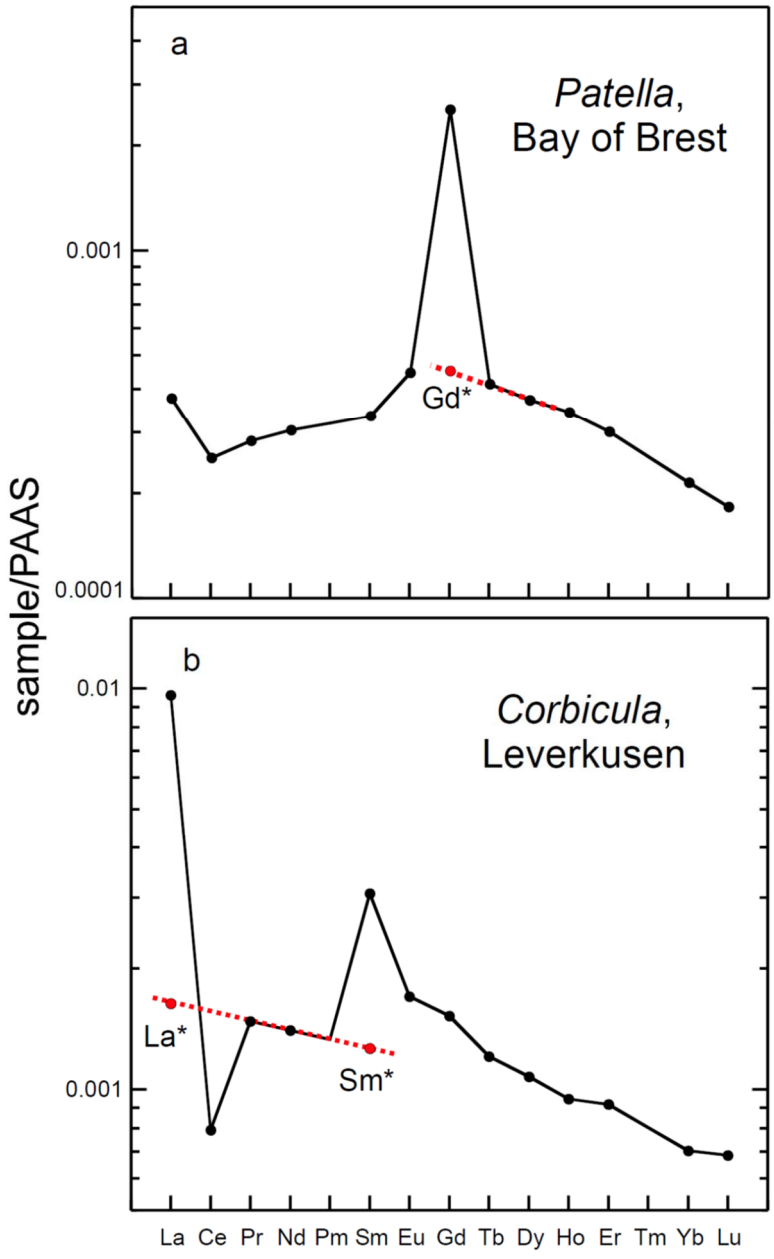

Figure 7. PAAS-normalized REE patterns of (a) a limpet shell (Le Goff et al., 2019) displaying a huge Gd anomaly (a), and (b) of a *Corbicula* shell displaying large La and Sm anomalies (Merschel and Bau, 2015). The red dotted lines show possible ways to estimate La*, Sm* and Gd* values. Note that the y-axis is logarithmic.

Figure 7a features a pattern of shell from the Bay of Brest (*Patella vulgata*; Le Goff et al., 2019), representing an excess Gd anomaly generated by the release of urine into coastal seawater, following injection of Gd-based contrast agents (Le Goff et al., 2019). Gadolinium is practically the sole REE contained in these products, although other REEs and Y can be also present in trace amounts (Veiga et al., 2020; Ben Salem and Barrat, 2021). This pollution does not generate other anomalies. Estimation of Gd* concentrations (i.e. the non-anthropogenic Gd concentration in the sample) can be made using the abundances of neighboring REEs, except for Eu as its relative abundance compared to other rare REEs can fluctuate (see above discussion). We can propose at least three ways of estimating Gd* by interpolating it with Sm and Tb (equation 6), by extrapolating from Nd and Sm (equation 7), or Tb and Dy (equation 8).

$$Gd/Gd^* = Gd_n / (Sm^{1/3} \times Tb_n^{2/3}) \quad \text{(equation 6)}$$

$$Gd/Gd^* = Gd_n \times Nd_n^2 / Sm_n \quad \text{(equation 7)}$$

$$Gd/Gd^* = Gd_n \times Dy_n / Tb_n^2 \quad \text{(equation 8)}$$

Note again that for equation 7, the existence of Pm cannot be omitted. Depending on the shape of the pattern, equation 8 seems one of the best choices here.

Nevertheless, REE pollution may be much more complex. For example, the shell of a bivalve taken from the Rhine near Leverkusen (Germany; Merschel and Bau, 2015) displays distinctive anomalies in both La and Sm (Fig. 7b). Despite its apparent simplicity, this case study illustrates the difficulties that environmental geochemists will have to overcome in the next few years due to enhanced REE pollution issues. First, it is certain that the La excess is here anthropogenic, since this anomaly is not present in the unpolluted waters of the Rhine (Kulaksiz and Bau, 2011, 2013). It can be estimated in the same way as above, using Pr and Nd (equation 5). The Sm anomaly is also of anthropogenic origin and probably linked to effluents discharged upstream by the same industry (Kulaksiz and Bau, 2013). It is possible that this industry also discharges other REE. However, these additional REE pollutants do not produce any marked anomalies here, but we cannot rule out the possibility that the anthropogenic contribution is "hidden" but not negligible elsewhere in the REE pattern, in agreement with Merschel and Bau (2015). In other words, Sm* must be estimated from

elements unaffected by pollution. We could choose elements heavier than Sm to extrapolate Gd*, but this seems rather uncertain here. We have already expressed our reservations about Eu. There is also a Gd anomaly here, and the Rhine is also contaminated with GBCA. We must therefore rely on the lighter elements, and once again on Pr and Nd, to interpolate Sm*, but we cannot know a priori whether these elements are not also affected by pollution. Using these two elements, the Sm anomaly could be estimated with the following equation:

$$Sm/Sm^* = Sm_n \times Pr_n^2 / Nd_n^3 \qquad \text{(equation 9)}$$

7/ REE patterns as a tool to evaluate data quality

We have summarized above the general principles that have led geochemists and cosmochemists to adopt REE patterns over the last decades. The REE distribution patterns in living organisms are also controlled by the same properties, reflecting the characteristics of their source material (e.g., seawater, nutrients), hence also justifying their use by biochemists and ecotoxicologists to present and interpret REE data. Importantly, these diagrams can be first used to assess the overall quality of measured data, and to identify results that are not reliable. The Oddo-Harkins effect is universal and also applies to the distribution of REEs in organisms, which means that smooth patterns are expected when normalizing a set of REE values to a chondritic or shale reference, except for potential REE anomalies in the event of anthropogenic pollution (Gd, Sm, etc.) or specific microbiological use (e.g., La, Ce, Eu). Living organisms (and the samples derived from them) are often depleted in REEs, and accurate determination of their abundances can be extremely difficult, if not a real analytical challenge. Below, we discuss selected patterns from recently published studies in order to illustrate how analytical problems can be detected (Fig. 8-9):

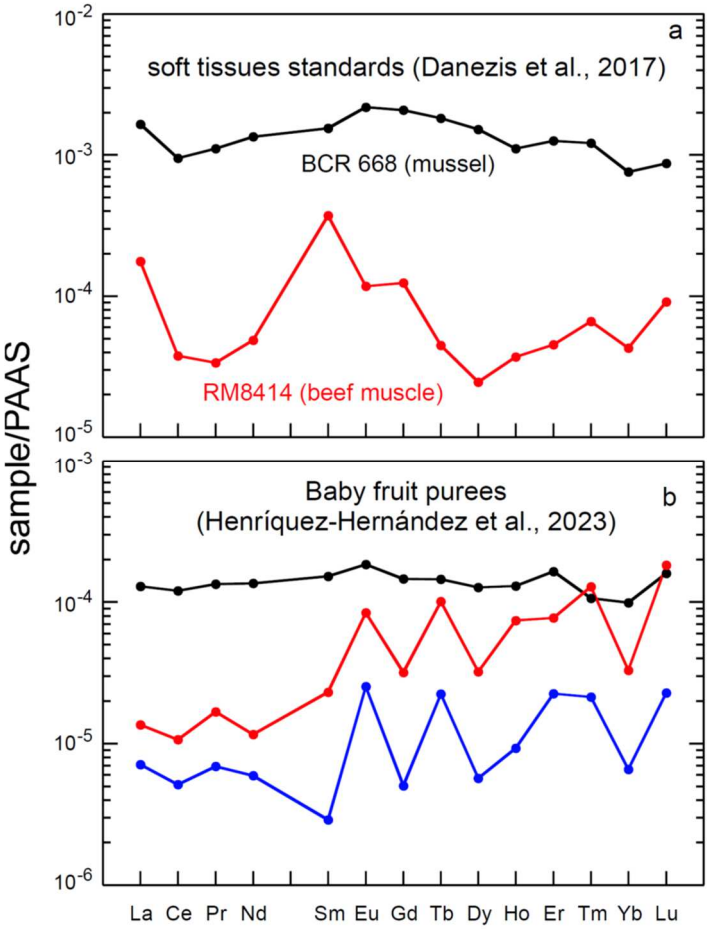

Figure 8. a: PAAS-normalized REE patterns of some reference materials prepared with soft tissues (Danezis et al., 2017); b: PAAS-normalized REE patterns of selected ready-to-eat fruit purees (Henríquez-Hernández et al., 2023).

- There is very limited data published so far for soft tissue standards and an effort should be made in the near future to develop and characterize reference tissues in order to validate REE data obtained on organic materials. Danezis et al (2017) analyzed two standards, a mussel soft tissue and a beef muscle (Fig. 8a). Their results for the mussel tissue (BCR 668) are very satisfactory, and similar to certified values. The shape of the obtained pattern is similar to that of bivalve tissues measured elsewhere (e.g., Wang et al., 2020; Castro et al., 2023), exhibiting for instance a small positive anomaly in La characteristic of a seawater origin. On the other hand, the resulting REE pattern identifies small negative anomalies in Ho and Yb that have never been identified in the marine environment so far. Considering the analytical difficulty of measuring accurate and precise REE abundances for such material, these anomalies are probably not real and therefore should not be overemphasized. Determining REE abundances

621 in the beef muscle standard (RM8414) is even more difficult considering that REE
622 concentrations are an order of magnitude lower. The REEs accumulated in a bovine's muscles
623 most likely derive from nutritional inputs and additional feed supplements. Although no
624 indication is available on this subject, it is reasonable to assume that the animal was fed
625 mainly with plant-derived products, whose compositional elements ultimately derive from
626 soils. One can presume that the REE patterns for these products must be similar to the upper
627 continental crust, hence being most likely similar to a shale reference (e.g., PAAS). Instead,
628 the obtained results show a very large positive La anomaly, together with notable enrichments
629 in middle REEs (Sm, Eu, Gd) and negative anomalies in Dy and Yb. Such REE anomalies are
630 unlikely, as they would imply unknown processes of biological REE fractionation. The
631 problem highlighted here is probably analytical, suggesting that the procedure used in that
632 particular study did not allow for REEs in this type of matrix to be quantified with sufficient
633 accuracy at such low concentrations.

634 - REEs are also frequently measured in food. Figure 8b presents selected REE patterns for
635 ready-to-eat baby fruit purees (Henríquez-Hernández et al., 2023). The reported REE
636 concentrations are very low, and their determination is therefore particularly challenging. The
637 sample exhibiting the greatest REE levels in that study exhibits a rather flat PAAS-normalized
638 pattern. As these purees are essentially made from vegetal products (fruit, sugar) grown on
639 soils derived from chemical weathering of continental rocks, a shale-like pattern was indeed
640 expected. However, this pattern shows discrepancies for the heaviest REEs, most likely of
641 analytical origin. Furthermore, the most REE-depleted samples show irregular patterns
642 exhibiting hectic anomalies, which clearly show that the technique used in that particular
643 study did not allow the determination of reliable REE abundances for such low concentration
644 levels. While the results obtained can be used to infer overall REE abundances in the order of
645 $< 10^{-4}$ x PAAS, they do not allow discussing the shape of REE pattern in these particular
646 samples. From a toxicological point of view, the conclusions drawn by the authors are valid.
647 However, these data should not be included in future databases to discuss pollution or
648 pollution emergence, since they are not sufficiently accurate, and since the resulting
649 anomalies are artifacts.

650

651

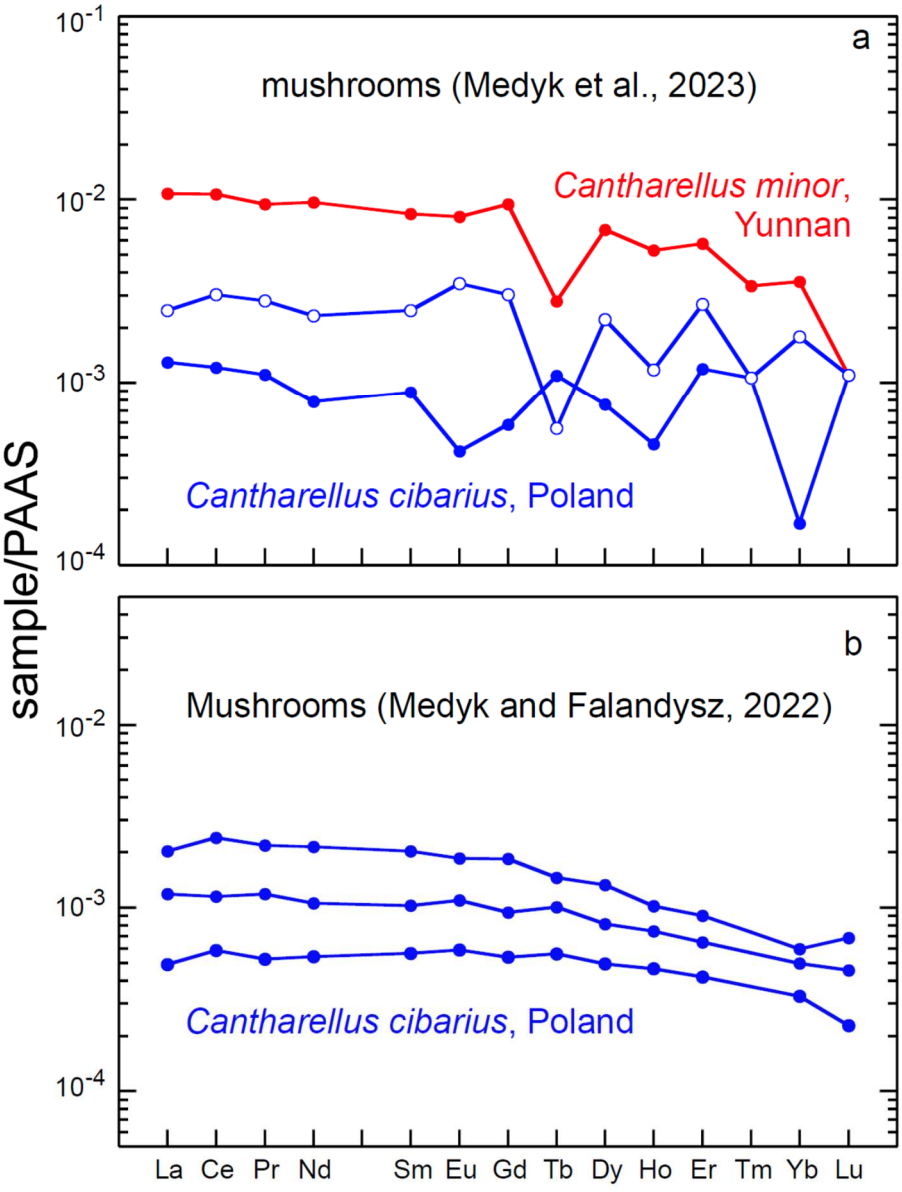

Figure 9. PAAS-normalized REE patterns of selected mushrooms from Poland and Yunnan. Data from Mędyk and Falandysz (2022) and Mędyk et al. (2023).

-The distribution of REEs in mushrooms mostly reflects the composition of soils on which they grow (Zocher et al., 2018). Mędik et al. (2023) have analyzed numerous chanterelle samples from China and Poland, whose REE spectra show pronounced anomalies, particularly for heavy REEs (Fig. 9a). Negative Tb and Yb anomalies were obtained in these samples, but they are most likely unreal since no negative Tb anomalies have ever been reported in continental crust rocks and extraterrestrial material. Ytterbium anomalies are also unknown in terrestrial rocks, and have only been encountered in a few primitive meteorites formed at very low fO_2 (e.g., Crozaz and Lundberg, 1995; Barrat et al., 2014). Additional analyses of Polish

mushrooms have been carried out by Mędyk and Falandysz (2022) using a chemical protocol adapted for low-level samples (i.e. after separation of REEs by ion-exchange chromatography), and the resulting patterns were correct (Fig. 9b).

These few examples demonstrate the utility of REE patterns not only for representing data, but also for detecting analytical problems or limitations. Detecting positive or negative anomalies for REEs in low-level organic samples requires high-quality measurements, validated by analyses of well-characterized reference materials. Efforts in this area are therefore needed, as standards of organic matter are currently insufficiently characterized.

8/ Perspectives

The REE patterns have been the tool of reference for representing REE data in earth sciences and cosmochemistry for over fifty years. While the number of studies using REE in ecotoxicology or biology has increased considerably in recent years, researchers in these fields have not yet fully adopted them. Other representations are used, but have many drawbacks. While they enable concentration levels to be visualized, they do not allow for a careful assessment of data quality, the determination of anomalies or of any general decoupling of certain elements relative to other REEs in studied samples. The aim of this paper was to explain the general principles and main properties of these diagrams, originally developed for rocks, so that they can be better understood by researchers initiating work on biological materials.

Until recently, it was extremely difficult to obtain reliable data on biological materials, given their low concentrations and the cumbersome techniques required to carry out such analyses. The development of ICP-MS has made it possible to obtain high-quality data on this type of material, opening up new fields of research. Moreover, with the increasing consumption of REEs by the industry and other human activities, these elements have now become emerging pollutants whose impact on ecosystems and the natural environment needs to be carefully investigated.

At present, a substantial effort is required to better characterize REE abundances in living organisms and to identify corresponding biological pathways. In other words, are REEs involved in metabolic reactions or not? Do they accumulate in certain organs? The recent discovery of the importance of certain REEs in the metabolism of methanotrophic species and

siderophores has shown that biological fractionation of REE is possible (e.g., Semrau et al., 2018; Wang et al., 2020; Kraemer and Bau, 2022), which should be further investigated in future studies. Similarly, the mechanism of transfer of the REEs from one trophic level to another, possibly associated with potential accumulation effects and decoupling, must also be evaluated (e.g., Marginson et al., 2023), together with the possible impact of biological and microbiological processes on the oceanic REE cycle or on their distribution in soils and terrestrial surface environments. These studies are also directly relevant to various environmental issues regarding the impact of pollution on ecosystems, hence the need to further develop ecotoxicological studies in the future in order to identify emerging REE pollutants. For these reasons, REE patterns will certainly become an essential tool for researchers working on these issues.

Acknowledgements.

We thank Milena Horvat for the editorial handling, and the two anonymous reviewers for their constructive reviews, and Richard C. Greenwood (Open University) for discussion.

References

Barrat J.A., Keller F., Amossé J., Taylor R.N., Nesbitt R.W., Hirata T. (1996) Determination of rare earth elements in sixteen silicate reference samples by ICP-MS after Tm addition and ion exchange separation. *Geostandards Newsletter* **20**, 1, 133-140.

Barrat J.A., Zanda B., Moynier F., Bollinger C., Liorzou C., and Bayon G. (2012) Geochemistry of CI chondrites: Major and trace elements, and Cu and Zn isotopes. *Geochim. Cosmochim. Acta* **83**, 79-92.

Barrat, J.A., Zanda, B., Jambon, A., Bollinger, C. (2014) The lithophile trace elements in enstatite chondrites. *Geochim. Cosmochim. Acta.* **128**, 71-94.

Barrat J.A., Dauphas N., Gillet P., Bollinger C., Etoubleau J., Bischoff A., Yamaguchi A. (2016) Evidence from Tm anomalies for non-CI refractory lithophile element proportions in terrestrial planets and achondrites. *Geochim. Cosmochim. Acta*, **176**, 1-17.

Barrat J.A., Bayon G., Carney R.S., Chauvaud L. (2022a) Rare earth elements as new biogeochemical proxies in deep-sea mussels. *Chem. Geol*., https://doi.org/10.1016/j.chemgeo.2022.121102.

Barrat J.A., Chauvaud L., Olivier F., Poitevin P., Bayon G., Ben Salem D. (2022b) Rare earth elements and yttrium in suspension-feeding bivalves (dog cockle, *Glycymeris glycymeris* L.): accumulation, vital effects and pollution. *Geochim. Cosmochim. Acta* **339**, 12-21.

Barrat J.A., Bayon G., Lalonde S. (2023) Calculation of cerium and lanthanum anomalies in geological and environmental samples, *Chem. Geol* **615**, 121202, https://doi.org/10.1016/j.chemgeo.2022.121202.

Bau M. (1996). Controls on the fractionation of isovalent trace elements in magmatic and aqueous systems: evidence from Y/Ho, Zr/Hf, and lanthanide tetrad effect. *Contrib. Mineral. Petrol.* **123**, 323-333.

Bau M., Dulski P. (1996a) Distribution of yttrium and rare earth elements in the Penge and Kuruman iron-formations,Transvaal Supergroup, South Africa. *Precambrian Research* **79**, 37-55.

Bau M., Dulski P. (1996b) Anthropogenic origin of positive gadolinium anomalies in river waters. *Earth Planet Sci. Lett.* **143**, 245-255.

Bau M., Möller P., Dulski P. (1997) Yttrium and lanthanides in eastern Mediterranean seawater and their fractionation during redox-cycling. *Marine Chemistry* **56**, 123-131.

Bau M., Balan S., Schmidt K., Koschinsky A. (2010) Rare earth elements in mussel shells of the *Mytilidae* family as tracers for hidden and fossil high-temperature hydrothermal systems. *Earth Planet. Sci. Lett.* **299**, 310-316.

Bau M., Schmidt K., Pack A., Bendel V., Kraemer D. (2018) The European Shale: an improved data set for normalisation of rare earth element and yttrium concentrations in environmental and biological samples from Europe. *Appl. Geochem.* **90**, 142-149.

Bayon G., Toucanne S., Skonieczny C., André L., Bermell S., Cheron S., Dennielou B., Etoubleau J., Freslon N., Gauchery T., Germain Y., Jorry S., Ménot G., Monin L., Ponzevera E., Rouget M.L., Tachikawa K., Barrat J.A. (2015) Rare earth elements and neodymium isotopes in World river sediments revisited. *Geochim. Cosmochim. Acta* **170**, 17-38.

Bayon G., Lemaitre N., Barrat J.A., Wang X., Feng D., Duperron S. (2020) Microbial utilization of rare earth elements at cold seeps related to aerobic methane oxidation. *Chem. Geol.* **555**, 119832.

Bellefroid E.J., Hood A.V.S., Hoffman P.F., Thomas M.D., Reinhard C.T., Planavsky, N.J. (2018) Constraints on Paleoproterozoic atmospheric oxygen levels. *PNAS* **115**, 8104-8109.

Ben Salem D., Barrat J.A. (2021) Determination of rare earth elements in gadolinium-based contrast agents by ICP-MS, *Talanta* **221**, 121589.

Brewer A., Dror I., Berkowitz B. (2022) Electronic waste as a source of rare earth element pollution: Leaching, transport in porous media, and the effects of nanoparticles. *Chemosphere* **287**, 132217.

Castro L., Farkas J., Munro Jenssen B., Piarulli S., Ciesielski T.M. (2023) Biomonitoring of rare earth elements in Southern Norway: Distribution, fractionation, and accumulation patterns in the marine bivalves *Mytilus spp.* and *Tapes spp.* . *Environmental Pollution* **335**, 122300.

Charles C., Barrat J.A., Pelleter E. (2021) Trace Element Determinations in Fe-Mn Oxides by High Resolution ICP-MS after Tm Addition. *Talanta* 122446.

Chayla B., Jaffrezic H., Joron J.L. (1973) Analyse par activation dans les neutrons épithermiques: Application à la détermination d'éléments traces dans les roches. *C. R. Acad. Sci. Paris* **277**, 273-275.

Coryell C.D., Chase J.W., Winchester J.W. (1963) A procedure for geochemical interpretation of terrestrial rare-earth abundance patterns. *J. Geophys. Res.* **68**, 559-566.

Crozaz, G., Lundberg, L.L. (1995) The origin of oldhamite in unequilibrated enstatite chondrites. *Geochim. Cosmochim. Acta* **59**, 3817-3831.

Danezis G.P., Pappas A.C., Zoidis E., Papadomichelakis G., Hadjigeorgiou I., Zhang P., Brusic V., Georgiou C.A. (2017) Game meat authentication through rare earth elements fingerprinting. *Analytica Chimica Acta* **991** (2017) 46-57.

Danezis G.P., Zoidis E., Zhang P., Pappas A.C., Tsagkaris A.S., Papachristidis C.A., Papadomichelakis G., Hadjigeorgiou I., Georgiou C.A. (2019) Tissue distribution of rare earth elements in wild, commercial and backyard rabbits. *Meat Sci.* **153**, 45-50.

Dang D.H., Ma L., Ha Q.K., Wang W. (2022) A multi-tracer approach to disentangle anthropogenic emissions from natural processes in the St. Lawrence River and Estuary. *Water Res.* **219**, 118588.

De Baar H.J.W., Bacon M.P., Brewer P.G., Bruland K.W. (1985) Rare earth elements in the Pacific and Atlantic Oceans. *Geochim. Cosmochim. Acta* **49**, 1943–1959.

Elderfield H., Upstill-Goddard R., Sholkovitz E.R. (1990) The rare earth elements in rivers, estuaries, and coastal seas and their significance to the composition of ocean waters. Geochim. Cosmochim. Acta, 54, 971-991.

Garcia-Solsona E., Jeandel C., Labatut M., Lacan F., Vance D., Chavagnac V., Pradoux C. (2014) Rare earth elements and Nd isotopes tracing water mass mixing and particle-seawater interactions in the SE Atlantic. *Geochim. Cosmochim. Acta* **125**, 351-372.

Gast P.W., Hubbard N.J., Wiesmann H. (1970) Chemical composition and petrogenesis of basalts from Tranquillity base. *Proc. First Lunar Sci. Conf., Geochim. Cosmochim. Acta,* Supp. 1, Vol. 2, 1143-1163.

Gaudry A., Zeroual S., Gaie-Levrel F., Moskura M., Boujrhal F.Z., El Moursli RC., Guessous A., Mouradi A., Givernaud T., Delmas R. (2007) Heavy metals pollution of the Atlantic marine environment by the Moroccan phosphate industry, as observed through their bioaccumulation in *Ulva lactuca*. *Water. Air. Soil Pollut.* **178**, 267-285.

German C.R., Elderfield H. (1990). Application of the Ce anomaly as a paleoredox indicator: the ground rules. *Paleoceanography* **5**, 823-833.

Goldberg E.D. (1961) Chemistry in the oceans, in: Oceanography, M. Sears, ed., *Am. Assoc. Adv. Sci. Publ.* **67**, 583-597.

Goldschmidt V.M. (1958) Geochemistry. Oxford Univ. Press, London, 730 pp.

Grenier M., Garcia-Solsona E., Lemaitre N., Trull T.W., Bouvier V., Nonnotte P., Souhaut M., Lacan F., Jeandel C. (2018) Differentiating lithogenic supplies, water mass transport, and biological processes on and off the Kerguelen Plateau using rare earth element concentrations and neodymium isotopic compositions. *Front. Mar. Sci.* 5, 426.

Gromet L.P., Haskin L.A., Korotev R.L. and Dymek R.F. (1984). The 'north American shale composite': its compilation, major and trace element characteristics. *Geochim. Cosmochim. Acta* **48**, 2469-2482.

Hatch G.P. (2012) Dynamics in the global market for rare earths. *Elements* **8**, 341-346.

Henderson P. (1984) General geochemical properties and abundances of the rare earth elements, in: P. Henderson (Ed.), Rare Earth Element Geochemistry, Elsevier, pp. l–32.

Henríquez-Hernández L.A., Acosta-Dacal A.C., Boada L.D., Zumbado M., Serra-Majem L., Luzardo O.P. (2023) Concentration of essential, toxic, and rare earth elements in ready-to-eat baby purees from the spanish market. *Nutrients* **15**, 3251.

Jahn B., Pol A., Lumpe H., Barends T.R., Dietl A., Hogendoorn C., Op den Camp H.J.M., Daumann, L.J. (2018) Similar but not the same: first kinetic and structural analyses of a methanol dehydrogenase containing a europium ion in the active site. *ChemBioChem* **19**, 1147-1153.

Jarvis I. and Jarvis K.E. (1992) Plasma spectrometry in the earth sciences: techniques, applications and future trends. *Chem. Geol.* **95**, 1-33.

Jenner G.A., Longerich H.P., Jackson S.E. and Fryer B.J. (1990) ICP-MS -A powerful tool for high-precision trace element analysis in Earth sciences: Evidence from analysis of selected U.S.G.S. reference samples. *Chem. Geol.* **83**, 133-148.

Johannesson K.H., Stetzenbach K.J., Hodge V.F. (1997) Rare earth elements as geochemical tracers of regional groundwater mixing. *Geochim. Cosmochim. Acta* **61**, 3605-3618.

Jochum K.P., Weis U., Schwager B., Stoll B., Wilson S.A., Haug G.H., Andreae M.O., Enzweiler J. (2016) Reference values following ISO guidelines for frequently requested rock reference materials, *Geostand. Geoanal. Res*. **40**, 333-350.

Kamber B.S., Webb G.E. (2001) The geochemistry of late Archaean microbial carbonate: Implications for ocean chemistry and continental erosion history. *Geochim. Cosmochim. Acta* **65**, 2509-2525.

Kamber B.S., Greig A., Collerson K.D. (2005) A new estimate for the composition of weathered young upper continental crust from alluvial sediments, Queensland, Australia, *Geochem. Cosmochim. Acta* **69**, 1041–1058.

Karamalidis A.K., Torres S.G., Hakala J.A., Shao H., Cantrell K.J., Carrol S. (2013) Trace metal source terms in carbon sequestration environments. *Environ. Sci. Technol.* **47**, 322-329.

Kraemer D., Bau M. (2022) Siderophores and the formation of cerium anomalies in anoxic environments. *Geochem. Persp. Let*. **22**, 50-55.

Kulaksiz S., Bau M. (2011) Rare earth elements in the Rhine River, Germany: first case of anthropogenic lanthanum as a dissolved microcontaminant in the hydrosphere. *Environ. Int.* **37**, 973–979.

Kulaksiz S., Bau M. (2013) Anthropogenic dissolved and colloid/nanoparticle-bound samarium, lanthanum and gadolinium in the Rhine River and the impending destruction of the natural rare earth element distribution in rivers. *Earth Planet. Sci. Lett.* **362**, 43–50.

Lawrence M.G., Greig A., Collerson K.D., Kamber B.S., (2006) Rare Earth Element and Yttrium variability in South East Queensland Waterways. *Aquat. Geochem.* **12**, 39–72.

Le Goff S, Barrat J.A., Chauvaud L., Paulet Y.M., Gueguen B., Ben Salem D. (2019) Compound-specific recording of gadolinium pollution in coastal waters by great scallops. *Scientific Reports* **9**, 8015.

Makishima A. and Nakamura E. (2006) Determination of major, minor and trace elements in silicate samples by ICP-QMS and ICP-SF-MS applying isotope dilution-internal standardization (ID-IS) and multi-stage internal standardisation. *Geostand. Geoanal. Res.* **30**, 245–271.

Marginson H., MacMillan G.A., Grant E., Gérin-Lajoie J., Amyot M. (2023) Rare earth element bioaccumulation and cerium anomalies in biota from the Eastern Canadian subarctic (Nunavik). *Sci. Total Env.* **879**, 163024.

Massari S., Ruberti M. (2013) Rare earth elements as critical raw materials: Focus on international markets and future strategies. *Resources Policy* **38**, 36-43.

Masuda, A. (1962) Regularities in variation of relative abundances of Lanthanide elements and an attempt to analyse separation index patterns of some minerals. *J. Earth Sci. Nagoya Univ*. **10**, 173-187.

Mędyk M., Falandysz J. (2022) Occurrence, bio-concentration and distribution of rare earth elements in wild mushrooms. *Sci. Total Env.* **851**, 158159.

Mędyk M., Falandysz J., Chidi Nnorom I. (2023) Scandium, yttrium, and lanthanide occurrence in *Cantharellus cibarius* and *C. minor* mushrooms. *Env. Sci. Poll. Res.* **30**, 41473-41484.

Merschel G., Bau M. (2015). Rare earth elements in the aragonitic shell of freshwater mussel *Corbicula fluminea* and the bioavailability of anthropogenic lanthanum, samarium and gadolinium in river water. *Sci. Total Environ.* **533**, 91-101.

Minster J.F., Allègre C.J. (1978) Systematic use of trace elements in igneous processes. *Contr. Mineral. Petrol.* **68**, 37-52.

Nance W.B., Taylor S.R. (1976) Rare earth element patterns and crustal evolution–I. Australian post-Archean sedimentary rocks. *Geochim. Cosmochim. Acta* **40**, 1539-1551.

Noack C.W., Dzombak D.A., Karamalidis A.K. (2014) Rare earth element distributions and trends in natural waters with a focus on groundwater. *Environ. Sci. Technol.* **48**, 4317-4326.

Nozaki Y., Zhang J., Amakawa H. (1997). The fractionation between Y and Ho in the marine environment. *Earth Planet. Sci. Lett*. **148**, 329-340.

Ouyang J., Wang X., Zhao B., Yuan X., Yuchun Wang Y. (2003) Effects of rare earth elements on the growth of *Cistanche deserticola* cells and the production of phenylethanoid glycosides. *J. Biotechnology* **102**, 129-134.

Ozaki T., Enomoto S., Minai Y., Ambe S., Ambe F., Tominaga T. (1997) Determination of lanthanides and other trace elements in ferns by instrumental neutron activation analysis. *J Radioanal Nucl Chem* **217**, 117-124.

Pack A., Russell S. S., Shelley J. M. G. and van Zuilen M. (2007) Geo- and cosmochemistry of the twin elements yttrium and holmium. *Geochim. Cosmochim. Acta* **71**, 4592–4608.

Pol, A., Barends, T.R.M., Dietl, A., Khadem, A.F., Eygensteyn, J., Jetten, M.S.M., Op den Camp, H.J.M. (2014) Rare earth metals are essential for methanotrophic life in volcanic mudpots. *Environ. Microbiol.* **16**, 255-264.

Pourmand, A., Dauphas, N., Ireland, T.J. (2011) A novel extraction chromatography and MC-ICP-MS technique for rapid analysis of REE, Sc and Y: Revising CI-chondrite and Post-Archean Australian Shale (PAAS) abundances. *Chem. Geol.* **291**, 38-54.

Pourret O., van der Ent A., Hursthouse A., Irawan D.E., Liu H., Wiche O. (2022) The 'europium anomaly' in plants: facts and fiction. *Plant Soil* **476**, 721-728.

Prudêncio M.I., Valente T., Marques R., Sequeira Braga M.A., Pamplona J. (2015) Geochemistry of rare earth elements in a passive treatment system built for acid mine drainage remediation. *Chemosphere* **138**, 691-700.

Schnetzler C.C., and J. A. Philpotts (1968) Partition coefficients of rare-earth elements and barium between igneous matrix material and rock- forming-mineral phenocrysts-I in Origin and Distribution of the Elements, vol. 30, edited by L. H. Ahrens, pp. 929-937, Pergamon Press.

Semrau J.D., DiSpirito A.A., Gu W., Yoon S. (2018) Metals and methanotrophy. *Appl. Environ. Microbiol.* **84**, e02289-17.

Shannon R.D. (1976). Revised effective ionic radii and systematic studies of interatomic distances in halides and chalcogenides. *Acta Crystallographica*, Section A, **32**, 751-767.

Shiller A.M., Chan E.W., Joung D.J., Redmond M.C., Kessler J.D. (2017) Light rare earth element depletion during Deepwater Horizon blowout methanotrophy. *Sci. Rep.* **7**, 10389.

Taylor S., McLennan S. (1985) The Continental Crust: Its Composition and Evolution. Blackwell Scientific Publications, 312 pp.

Tostevin R., Shields G.A., Tarbuck G.M., He T., Clarkson M.O., Wood R.A. (2016) Effective use of cerium anomalies as a redox proxy in carbonate-dominated marine settings. *Chem. Geol.* **438**, 146-162.

Veiga M., Mattiazzi P., de Gois J.S., Nascimento P.C., Borges D.L.G., Bohrer D. (2020) Presence of other rare earth metals in gadolinium-based contrast agents, *Talanta* **216**, 120940

Wallace M.W., Hood A.S., Shuster A., Greig A., Planavsky N.J., Reed C.P., (2017) Oxygenation history of the Neoproterozoic to early Phanerozoic and the rise of land plants. *Earth Planet. Sci. Lett.* **466**, 12-19.

Walsh J.N., Buckley F. and Barker J. (1981) The simultaneous determination of the rare earth elements in rocks using inductively coupled plasma source spectrometry. *Chem. Geol.* **33**, 141-153.

Wang X., Barrat J.A., Bayon G., Chauvaud L., Feng D. (2020) Lanthanum anomalies as fingerprints of methanotrophy. *Geochem. Persp. Let.* **14**, 26-30.

Watkins P.J. and Nolan J. (1992) Determination of rare earth elements, yttrium, scandium and hafnium using cation-exchange separation and inductively coupled plasma-atomic emission spectrometry. *Chem. Geol.* **95**, 131-139.

Wilkin R.T., Lee T.R., Ludwig R.D., Wadler C., Brandon W., Mueller B., Davis E., Luce D., Edwards T. (2021) REEs as natural tracers for in situ remediation of groundwater. *Environ. Sci. Technol.* **55**, 1251-1259.

Zepeda V.K., Kamber B.S. and Ghidan O.Y.A. (2023) Direct accurate Eu anomaly analysis in very high Ba/Eu silicate samples by triple-quadrupole ICP-MS in MS/MS mass shift mode, *Chem. Geol.*, https://doi.org/10.1016/j.chemgeo.2023.121827

Zocher A.L., Kraemer D., Merschel G., Bau M. (2018) Distribution of major and trace elements in the bolete mushroom Suillus luteus and the bioavailability of rare earth elements. *Chem. Geol.* **483**, 491-500.

Zocher A.L., Klimpel F., Kraemer D., Bau M. (2021) Assessing the bioavailability of dissolved rare earths and other trace elements: Digestion experiments with aquatic plant species *Lemna minor* ("duckweed" reference standard BCR-670). *Applied Geochemistry* **134**, 105025, https://doi.org/10.1016/j.apgeochem.2021.105025.

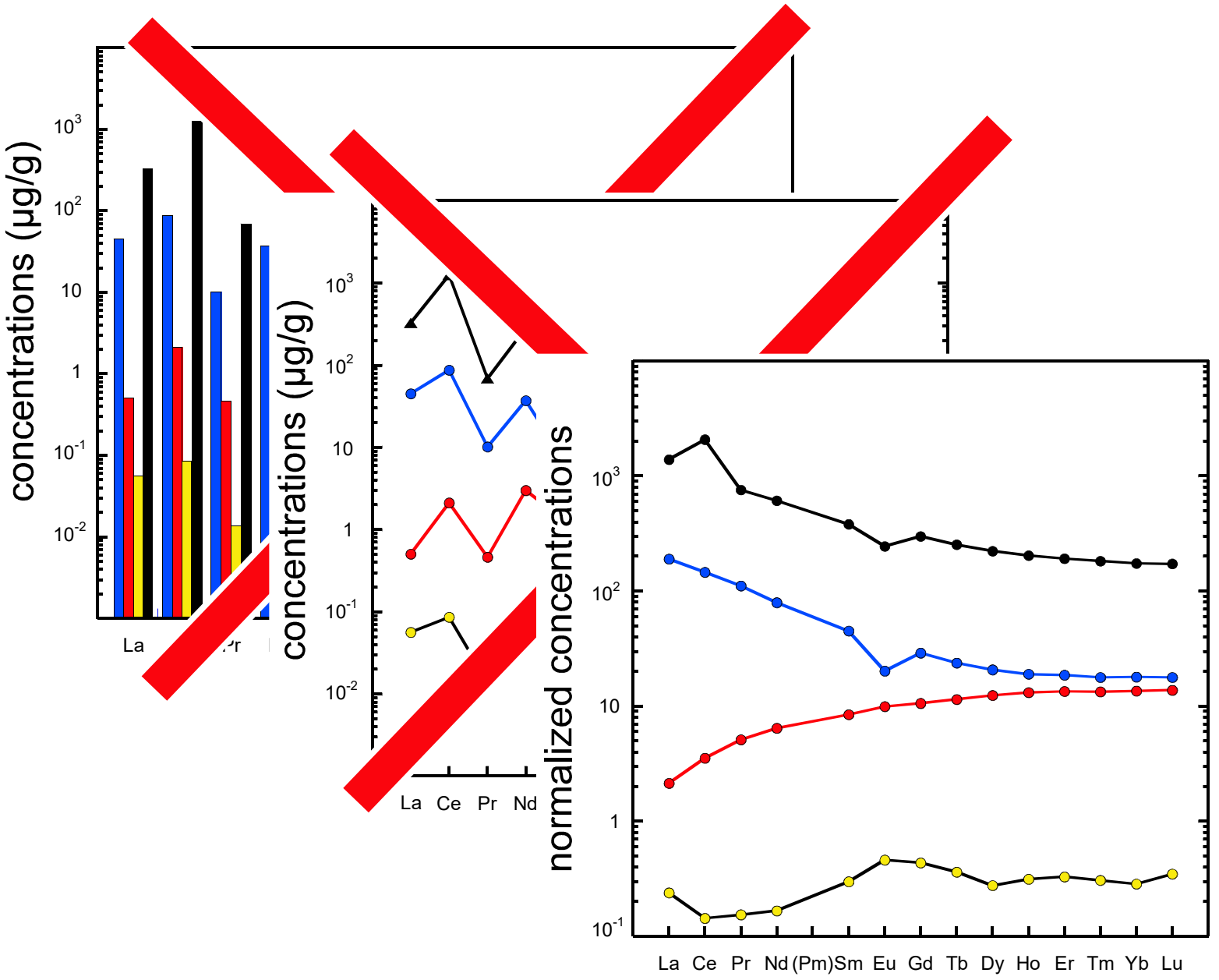
concentrations (μg/g)
10^3
10^2
10
1
10^{-1}
10^{-2}
La
concentrations (μg/g)
10^3
10^2
10
1
10^{-1}
10^{-2}
La Ce Pr Nd
normalized concentrations
10^3
10^2
10
1
10^{-1}
La Ce Pr Nd (Pm) Sm Eu Gd Tb Dy Ho Er Tm Yb Lu